Mechanisms of nitrous oxide (N_2O) formation and reduction in denitrifying biofilms

Sabba, Fabrizio; Picioreanu, Cristian; Nerenberg, Robert

DOI
10.1002/bit.26399

Publication date
2017

Document Version
Final published version

Published in
Biotechnology and Bioengineering

PHCbi

70% of surveyed scientists admitted that they could not replicate someone else's research.[1]

50% admitted that they couldn't replicate their own research.[1]

Stability, Reproducibility and Accuracy

The complete selection of PHCbi brand CO_2 and multigas incubators includes benchtop, stackable and reach-in models to meet a wide range of culture conditions, space needs and decontamination method preferences.

- Standard inCu-saFe® copper enriched germicidal surfaces prevent contamination before it starts
- Select models feature integrated dual high heat or H_2O_2 vapor and SafeCell™ UV scrubbing which combine to increase *in vitro* cell safety

We have an incubator that will meet your needs. Visit our overview, "Choosing Your Cell Culture Incubator" to help make your selection.

PHC Corporation of North America

PHC Corporation of North America
1300 Michael Drive, Suite A, Wood Dale, IL 60191
Toll Free USA (800) 858-8442, Fax (630) 238-0074
www.phchd.com/us/biomedical

1) Baker, Monya. "1,500 scientists lift the lid on reproducibility." Nature, no. 533 (May 26, 2016): 452-54. doi:10.1038/533452a.

Received: 24 March 2017 | Revised: 7 July 2017 | Accepted: 2 August 2017
DOI: 10.1002/bit.26399

ARTICLE

WILEY BIOTECHNOLOGY & BIOENGINEERING

Mechanisms of nitrous oxide (N_2O) formation and reduction in denitrifying biofilms

Fabrizio Sabba[1] | Cristian Picioreanu[2] | Robert Nerenberg[1]

[1] Department of Civil and Environmental Engineering and Earth Sciences, University of Notre Dame, Notre Dame, Indiana

[2] Department of Biotechnology, Faculty of Applied Sciences, Delft University of Technology, Delft, The Netherlands

Correspondence
Department of Civil and Environmental Engineering and Earth Sciences, University of Notre Dame, 156 Fitzpatrick Hall, Notre Dame, IN 46556.
Email: rnerenbe@nd.edu

Funding information
National Science Foundation, Division of Chemical, Bioengineering, Environmental, and Transport Systems, Grant number: CBET0954918; Water Environment Research Foundation, Grant number: U2R10

Abstract

Nitrous oxide (N_2O) is a potent greenhouse gas that can be formed in wastewater treatment processes by ammonium oxidizing and denitrifying microorganisms. While N_2O emissions from suspended growth systems have been extensively studied, and some recent studies have addressed emissions from nitrifying biofilms, much less is known about N_2O emissions from denitrifying biofilm processes. This research used modeling to evaluate the mechanisms of N_2O formation and reduction in denitrifying biofilms. The kinetic model included formation and consumption of key denitrification species, including nitrate (NO_3^-), nitrite (NO_2^-), nitric oxide (NO), and N_2O. The model showed that, in presence of excess of electron donor, denitrifying biofilms have two distinct layers of activity: an outer layer where there is net production of N_2O and an inner layer where there is net consumption. The presence of oxygen (O_2) had an important effect on N_2O emission from suspended growth systems, but a smaller effect on biofilm systems. The effects of NO_3^- and O_2 differed significantly based on the biofilm thickness. Overall, the effects of biofilm thickness and bulk substrate concentrations on N_2O emissions are complex and not always intuitive. A key mechanism for denitrifying biofilms is the diffusion of N_2O and other intermediates from one zone of the biofilm to another. This leads to zones of N_2O formation or consumption transformations that would not exist in suspended growth systems.

KEYWORDS
biofilms, denitrification, greenhouse gases, modeling, nitrous oxide

1 | INTRODUCTION

Wastewater treatment plants (WWTP) increasingly are using nitrification and denitrification to remove total nitrogen. Despite the environmental benefits of nitrogen removal, an unintended consequence is the formation of nitrous oxide (N_2O), a potent greenhouse gas and a strong ozone-depleting compound (Ravishankara, Daniel, & Portmann, 2009).

N_2O emissions from suspended growth systems have been extensively studied. A recent study suggested that ammonia oxidizing bacteria (AOB) in biofilms behave very differently than in suspended growth systems. This was not due to differences in the underlying microbial mechanisms of N_2O formation, but due to substrate gradients and diffusion of hydroxylamine, a nitrification intermediate, within the biofilm (Sabba, Picioreanu, Perez, & Nerenberg, 2015).

Less is known how the biofilm environment affects N_2O formation in denitrifying biofilms. This can be quite complex, given the large number of denitrification intermediates and potential gradients of oxygen and organic carbon within the biofilm. Since N_2O is an obligatory intermediate in the denitrification pathway, some N_2O always accumulates formed during denitrification. Higher rates of nitrate reduction usually result in higher N_2O concentrations, as

higher substrate concentrations are needed for higher enzymatic degradation rates (Law, Ye, Pan, & Yuan, 2012; Sutka et al., 2006; Zumft, 1997). Also, most denitrifiers can use N_2O as a sole external electron acceptor, and can reduce N_2O concurrently with nitrate (NO_3^-) or nitrite (NO_2^-) (Nielsen, Christensen, Revsbech, & Sorensen, 1990; Read-Daily, Sabba, Pavissich, & Nerenberg, 2016; Vilar-Sanz et al., 2013). Thus, depending on the conditions, denitrifying microorganisms may be a net source or a net sink of N_2O.

A few studies have addressed N_2O emissions from denitrifying biofilm processes. For example, Schreiber, Polerecky, and de Beer (2008) found that the characterization of micro-environmental conditions is needed to determine the potential source of N_2O production in complex and stratified environments. Eldyasti, Nakhla, and Zhu (2014) found that the biofilm thickness can play an important role in N_2O emissions. Research has also investigated the potential for NO_2^- accumulation in nitrifying and denitrifying systems, and found that high NO_2^- concentration in both cases can lead to higher N_2O emissions (Kampschreur, Temmink, Kleerebezem, Jetten, & van Loosdrecht, 2009; Lu & Chandran, 2010; Wu, Zheng, & Xing, 2014). However, these studies involved complex systems, in which the biofilm thicknesses, microbial composition, and substrate concentrations were not well characterized. Therefore the underlying mechanisms of N_2O emissions were not clear.

A number of studies have established the kinetics of N_2O formation and reduction by denitrifying bacteria (Read-Daily et al., 2016; von Schulthess, Kuhni, & Gujer, 1995; von Schulthess, Wild, & Gujer, 1994; Wicht, 1996; Wild, von Schulthess, & Gujer, 1994). While the behavior of denitrifying bacteria is in suspended growth systems can be gleaned from kinetics, the behavior of denitrifiers in biofilms is less obvious. Given substrate gradients in the biofilm, N_2O formed in one region may diffuse to others and be reduced.

Given the complexity of biofilms, modeling can be a useful tool to help understand the factors leading to N_2O emissions. A recent study from Sabba, Picioreanu, Boltz, and Nerenberg (2016) used modeling to predict N_2O emissions from nitrifying and denitrifying biofilm systems. However, this work did not systematically explore the underlying mechanisms of N_2O emissions, and did not assess the effects of COD limitation, the presence of O_2, or competing nitrogen oxides on N_2O emission by denitrifying biofilms.

Some researchers adapted the standard ASM models to include N_2O as a state variable, for example, (Hiatt & Grady, 2008; Kampschreur et al., 2012; Ni, Ruscalleda, Pellicer-Nacher, & Smets, 2011). However, they assumed that each nitrogen reductase acted independently of the others, and therefore donor limitation affected all reduction rates equally. Recent research suggests these models are not accurate when the production of reducing equivalents becomes rate limiting (Pan, Ni, & Yuan, 2013; Pan, Ni, Bond, Ye, & Yuan, 2013). A new modeling approach, called Activated Sludge Model with Indirect Coupling of Electrons (ASM-ICE), allows a better prediction and understanding of intermediates accumulation in biological denitrification (Pan et al., 2015). Previous modeling studies based on this novel approach were carried out to explore the mechanisms of N_2O emissions from nitrifying and denitrifying biofilms (Sabba et al., 2015, 2016).

Recently, Pan, Ni, and Yuan (2013) developed a simplified ICE model for heterotrophic denitrification (Figure 1). This approach may be especially useful for assessing N_2O emissions from denitrifying biofilms, where multiple acceptors may be present, and where the donor may become limiting in the deeper portions of biofilm. Therefore, in this study, we used numerical modeling based on the suspended growth kinetic model of Pan, Ni, and Yuan (2013) to assess N_2O formation in denitrifying biofilms, for a variety of bulk conditions and biofilm thicknesses.

In this research, we use a 1-D biofilm model with constant thickness to systematically explore N_2O formation and consumption. In particular, we explored the effects of bulk NO_3^- and DO on N_2O formation, either in presence of excess or limiting electron donor, and we evaluated the effects of biofilm thicknesses. We also considered the presence of influent N_2O.

2 | MATERIALS AND METHODS

2.1 | Denitrification model

The denitrification kinetic model was adapted from Pan, Ni, and Yuan (2013). The model stoichiometry, process rates, and parameters are summarized in Tables S1–S4 in the Supplementary Information. The model includes the reduction of NO_3^-, NO_2^-, NO, and N_2O, and the rate expressions are the product of maximum specific substrate utilization rates, biomass concentrations, Monod terms for donor or acceptor, as appropriate, and Monod term for M_{ox} or M_{red}, as appropriate. Pan, Ni, Bond, et al. (2013) determined parameters for a mixed-culture, carbon-oxidizing, denitrifying community, including affinity constants K_{Mox} for the donor and K_{Mred} for each substrate. All reduced and oxidized intracellular electron carriers are lumped into components M_{red} and M_{ox}, respectively. The use of M_{ox} and M_{red} as state variables, where the sum of the two remains constant, ensures a balance between oxidation and reduction rates. For example, if there is donor but no acceptor available, the M_{red} concentration will increase and the M_{ox} decrease until it becomes rate limiting, shutting down the donor oxidation rate. Key features of the model are described below, while an in-depth analysis of the denitrification model can be found in section S1 of the Supplementary Information.

Reactions r1 and r2 are donor oxidation rates, resulting in the formation of M_{red} and active biomass. In the conditions evaluated by Pan, Ni, Bond, et al. (2013), the maximum specific rate of reaction r1 (donor oxidation for energy) is 8.46 mmol g^{-1} h^{-1} (50.8 e^- eq g^{-1} hr^{-1}). Reaction r2 is the biomass synthesis, with the same maximum specific rate as r1, but with a specific stoichiometry for biomass synthesis. Reaction r3 is the reduction of NO_3^- to NO_2^-. This step has a relatively low maximum rate, 3.99 mmol g^{-1} hr^{-1} (3.99 e^- eq g^{-1} hr^{-1}), and high half saturation constant for M_{red} (4.58×10^{-3}). Reaction r4 is the reduction of NO_2^- to NO. This has a slightly higher maximum rate, 5.27 mmol g^{-1} h^{-1} (5.27 e^- eq g^{-1} hr^{-1}), and also the lowest half saturation constant for M_{red} (3.93×10^{-4}). Reaction r5 is the reduction of NO to N_2O. This step has a very high maximum rate, 50 mmol g^{-1} h^{-1} (25 e^- eq g^{-1} hr^{-1}), and low half saturation constant for M_{red} (1×10^{-3}).

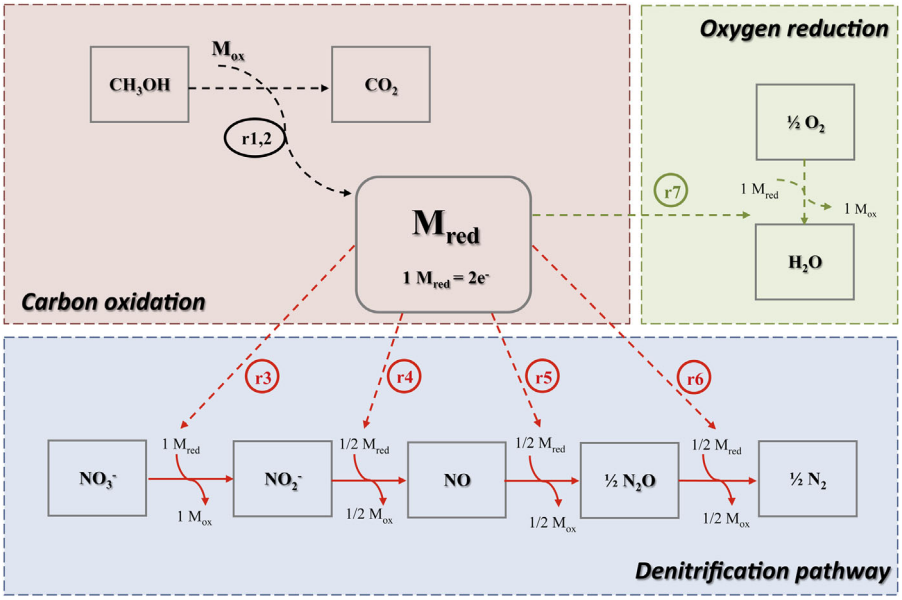

FIGURE 1 Schematic of the model for heterotrophic denitrification, adapted from Pan, Ni, and Yuan (2013). Arrows from the electron pool (represented by the reduced mediators, M_{red}) are electron-consuming processes. Arrows to the electron pool are electron-producing processes. The r terms in circles indicate the reaction rates. Details about the denitrification metabolic model can be found in section S1 in the Supplementary Information

NO is toxic to bacteria, and its reduction is very fast to minimize its accumulation. Reaction r5 is the reduction of N_2O to N_2. N_2O reduction also has a high maximum rate, 20 mmol g^{-1} h^{-1} (40 e^- eq g^{-1} hr^{-1}), and half saturation constant for M_{red} similar to that of NO_3^- (3.23×10^{-3}).

Our model includes O_2 reduction as an additional process that competes for electrons. Oxygen reduction is the rate expression r7. We assumed both a high maximum reduction rate of 50 mmol g^{-1} hr^{-1} (200 e^- eq g^{-1} hr^{-1}), and a low half saturation constant for M_{red} (1×10^{-6}). As long as O_2 is present at appreciable concentrations relative to K_{O_2} (6.25×10^{-3} mmol L^{-1}), the M_{red} will remain at very low levels, inhibiting the reduction of nitrogen oxides. From a modeling perspective, this behaves similarly to an "oxygen switch" $\left(K_{O_2}/K_{O_2} + S_{O_2}\right)$ used in the ASM models. As explained in S1 of the supplementary information, the exact value of the oxygen maximum specific reduction rate does not impact the predicted N_2O emissions, as long as the oxygen maximum specific reduction rate is higher than the COD maximum specific oxidation rate. In this case, the COD oxidation will be rate limiting.

2.2 | Biofilm model

The model assumed a 1-D biofilm without growth, decay, or detachment, in a well-mixed Continuous Stirred Tank Reactor (CSTR). This assumption of constant thickness was appropriate to explore the short-term response of a previously grown biofilm when subjected to different environmental conditions.

The model for N_2O production in denitrifying biofilms is based on mass balances for organic carbon, NO_3^-, NO_2^-, NO, N_2O, and O_2. Time-dependent mass balances in planar biofilms included net reaction rates for each soluble component, and effective diffusion coefficients of 50% that for the aqueous phase. The net component rates resulted from the process stoichiometry and kinetics from Pan, Ni, and Yuan (2013).

A zero-flux boundary for solutes was set at the base of the biofilm, and the concentration at the biofilm top surface equaled the bulk concentration, that is, the liquid boundary layer was neglected for simplicity. Finally, the concentrations of mediators, M_{red} and M_{ox}, in the biofilm were calculated from time-dependent balances that included reactions but not transport, that is, since mediators are internal to cells, they do not diffuse through the biofilm.

All model equations, process matrix, and complete list of parameters used for this model are provided in the Supplementary Information (sections S2–S4 and Tables S1–S3)

The cases evaluated in this study included a reactor hydraulic retention time (HRT) of 1.5 hr, biofilm specific surface area of 125 m^2 m^{-3}, planar biofilm thickness of 400 μm, biomass concentration in the biofilm of 10 g L^{-1}, bulk NO_3^- concentration variable between 0.001 and 40 mgN L^{-1}, and bulk DO variable between 0 and 1.2 mgO_2 L^{-1}.

The model was implemented in COMSOL Multiphysics (v4.4, Comsol, Inc., Burlington, MA) and solved with variable time step on a biofilm domain discretized with a mesh size of 1 μm. The reported results were for steady state. Gas stripping from bulk liquid (e.g., by aeration) was not included in this model. Gas stripping can increase transport of N_2O from the biofilm into the bulk liquid, but it is unlikely to have a significant effect on the rates of N_2O formation in the biofilm (Sabba et al., 2016).

2.3 | Sensitivity analysis

A sensitivity analysis was carried out for the assumed oxygen maximum reduction rate, q_{max,O_2} and oxygen half saturation constant for M_{red}, K_{Mred5}, (Supplementary Information—Figure S1). The parameters were left as in the base case, increased by 10%, or reduced by 10%. The N_2O emissions were not affected by the change in these parameters showing that the assumed values had negligible effects on the emissions.

3 | RESULTS

In this section, we first discuss the behavior of the kinetic model and the conditions that might lead to electron limitation. Then we use the model to assess two base cases to identify the basic mechanisms of N_2O formation in denitrifying biofilms. The base cases addressed a 400-μm thick biofilm with a bulk NO_3^- concentration of 14 mgN L^{-1}, and either anoxic bulk conditions or a bulk with 1.2 mgDO L^{-1}. The model was then used to systematically explore N_2O emissions as a function of bulk NO_3^- and DO for biofilms of different thicknesses. The thinnest biofilm of 5 μm was assumed to represent suspended growth.

3.1 | Mechanisms of N_2O formation

This section explores the biofilm mechanisms and conditions leading to N_2O production, considering a biofilm under two different scenarios: a purely denitrifying biofilm and a biofilm with an aerobic bulk (DO of 1.2 mg L^{-1}). In all cases, the biofilm thickness is 400 μm, the bulk NO_3^- concentration is 14 mgN L^{-1}, and the electron donor is non-rate-limiting throughout the entire biofilm. The NO concentrations and rates are not discussed in detail, as NO is quickly consumed and maintained at near-zero concentrations, and the rates are approximately equal to those of NO_2^- reduction. Note that "components" are state variables, and "component rates" are the net rates of transformation for each state variable, considering all the processes that produce or consume it. The "process rates" are the individual rates for each component, that is, the reaction rates r. Electron rates are the individual and aggregate rates of M_{red} formation and consumption from the different processes.

3.2 | Denitrifying biofilms with excess donor

When NO_3^- is supplied as the acceptor and the electron donor is present in excess (non-rate-limiting concentrations) throughout the biofilm, the biofilm activity can be divided into two zones: an exterior zone where there is net production of NO_2^- and N_2O, and an interior zone where there is net consumption of NO_2^- and N_2O (Figure 2a).

The outer biofilm is exposed to high NO_3^- concentrations, supplied from the bulk (Figure 2a). This leads to high rates of NO_3^- reduction (Figure 2c). In a suspended growth system, the NO_2^- and N_2O concentrations would increase until the reduction rates matches the formation rate based on NO_3^- reduction, as discussed in section 3.1. However, in the biofilm there is "leakage" of NO_2^-, NO, and N_2O to both the bulk liquid and the interior of the biofilm, as evidenced by the concentration gradient toward the bulk and interior (Figure 2a). The bulk is a sink because influent lacks NO_2^- and N_2O. The biofilm interior is a sink due to the biological reduction of NO_2^-, NO, and N_2O. This is because the interior has NO_3^- limitation and therefore less formation of NO_2^-, NO, and N_2O. As a result, NO_2^- and N_2O concentrations in the biofilm exterior are lower than needed to allow the NO_2^- reduction rate to match that of NO_3^-, and the N_2O reduction rate to match that of NO_2^-. Thus, there is net formation of NO_2^- and N_2O in the outer biofilm (Figure 2b).

Deeper in the biofilm, at around 300 μm, when both the NO_3^- concentration (Figure 2a) and the rate of NO_3^- reduction (Figure 2c) begin to decrease, the rate of NO_2^- reduction, r4, becomes higher than that of NO_3^- reduction, r3. This is due to the elevated NO_2^- concentration resulting from diffusion from the outer biofilm. A similar effect occurs with N_2O. Thus, the component rates for NO_2^- and N_2O become negative, explaining the sink for these compounds described above (Figure 2b). This can also be observed in Figure 2d, where the electron rates are highest for NO_3^- in the outer biofilm, but then become higher for NO_2^- and N_2O deeper in the biofilm. Thus, unlike a suspended growth system where the bulk liquid is the only sink for N_2O, the biofilm has an interior sink and reduced N_2O to N_2. Thus, denitrifying biofilms are likely to have lower bulk emissions of N_2O when carbon is in excess.

3.3 | Denitrifying biofilms with an aerobic bulk and excess donor

The mechanisms of N_2O formation change significantly when the bulk is aerobic. A key difference is that M_{red} (electron pool) becomes limiting in the outer biofilm due to the high rate of O_2 reduction. For a bulk DO of 1.2 mg L^{-1}, the bulk NO_2^- and N_2O concentrations are 0.066 and 0.072 mgN L^{-1}, respectively (Figure 2e). While the bulk NO_2^- concentration is lower than that calculated for an anoxic bulk liquid (Figure 2a), the bulk N_2O is around 11% higher.

In this case, the biofilm can be divided in four regions of activity: an outer, outer central, inner central, and inner portion. The inner two zones are similar to those described above, while the outer two zones are different.

The outer portion is dominated by O_2 reduction. This leads to low M_{red} concentrations and inhibition of denitrification, as expected (Figures 2e and 2f). In a narrow, outer central section of biofilm, around 320 μm, the O_2 concentration approaches zero (Figure 2e) and the M_{red} concentration begins to increase. In this zone, there is very little NO_3^- reduction, because it has a relatively low rate and low affinity for M_{red}. However, NO_2^- reduction has high affinity for electrons and NO_2^- can be consumed in this region. Since N_2O reduction has a lower affinity for M_{red}, there is net N_2O formation. This can be seen in in Figure 2f, where at around 320 μm there is a negative spike in the NO_2^- component rate (net reduction), and a positive spike in N_2O formation rate (net formation).

Deeper in the biofilm, below 320 μm, the O_2 concentration approaches zero and NO_3^- reduction occurs in a similar fashion to the

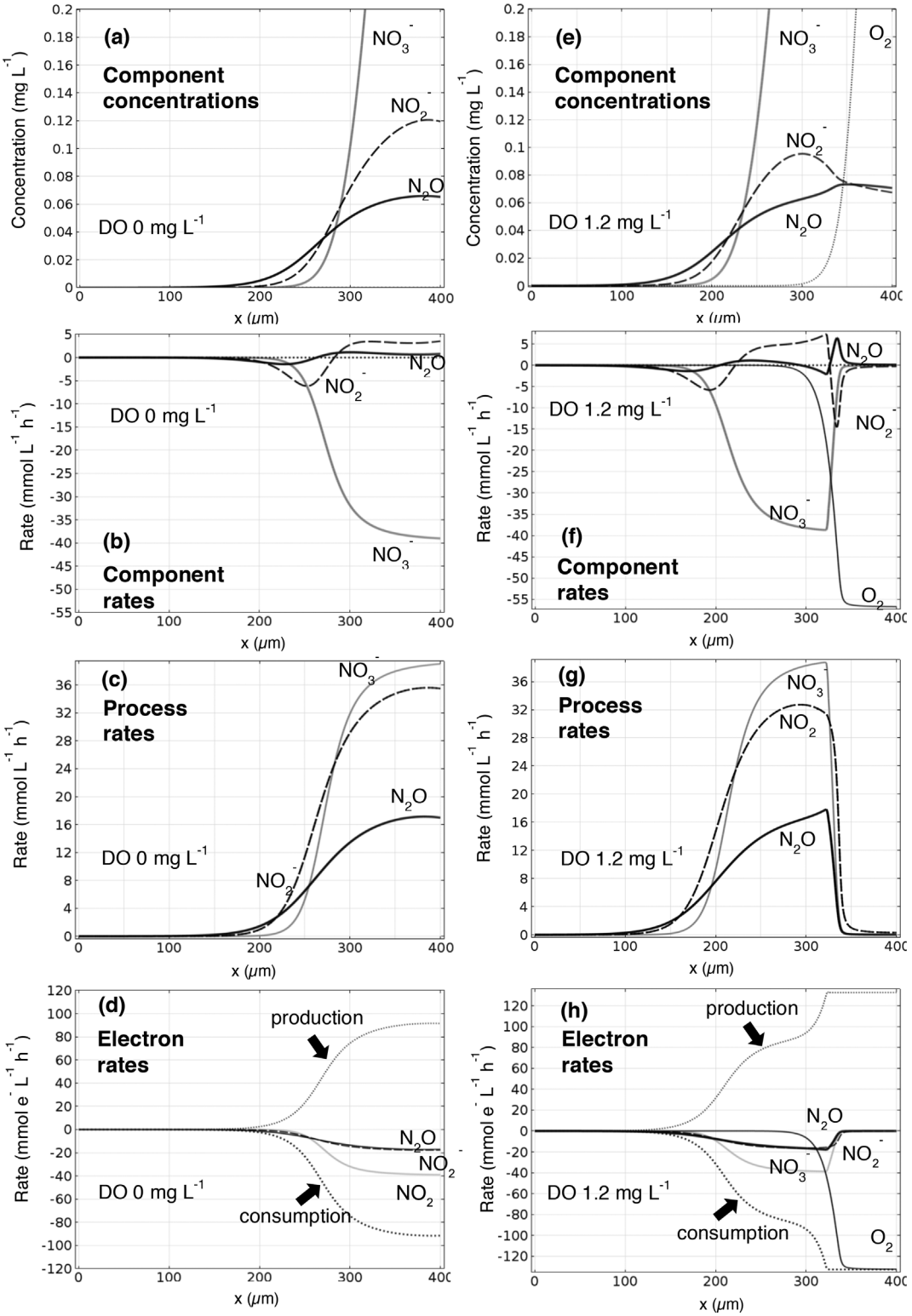

FIGURE 2 Concentration and rate profiles in a 400-μm biofilm with excess electron donor, either with an anoxic (a–d) or aerobic (e–h) bulk liquid. Component concentrations (a and e), net component reaction rates (b and g), process rates (c and f) and electron production/consumption rates (d and h) over the biofilm depth. All the results were obtained for the base case conditions

anoxic biofilm described above, with an outer zone forming NO_2^- and N_2O and in inner zone consuming them. A difference, though, is that the NO_2^- produced in the NO_3^- reduction zone has an additional sink toward the narrow, exterior central band described in the previous paragraph. The N_2O may be produced at higher concentrations than in the anoxic biofilm, due to higher NO_2^- reduction rates relative to NO_3^- reduction rates. This explains the higher N_2O concentration in the bulk. As opposed to the anoxic conditions (Figure 2b) where NO_2^- reduction

occurs around 280 μm, under oxic conditions NO_2^- is reduced at two different depths, around 220 μm and 350 μm (Figure 2b). The latter results in production of N_2O that, given the closer proximity to the bulk compared to the anoxic conditions (Figure 2b), is released in the bulk with higher N_2O emissions.

Note that in a suspended growth system, there would be little or no N_2O formation for an aerobic bulk, because there would be no denitrification. The biofilm not only allows denitrification with an aerobic bulk, but can increase N_2O formation and emission due to diffusion of intermediates from one zone of the biofilm to another.

3.4 | Denitrifying biofilms with electron donor limitation

The above scenarios assume the donor concentration is in excess, that is, much higher than its half saturation coefficient, K_S, throughout the biofilm. If the donor is limiting within the biofilm, for example approaching or below its K_S, it leads to M_{red} limitation in ways that differ from the M_{red} limitation caused by O_2. For example, when there is a low bulk electron donor concentration and no bulk O_2, there is some NO_3^- reduction in the outer biofilm, but the rates are lowered by the low M_{red} concentration, so little NO_2^- and N_2O are formed. There also is less N_2O reduction deeper in the biofilm, due to the even lower M_{red} concentration.

The model was used to estimate emissions in a 400 μm biofilm with limiting COD in absence of O_2. For this scenario the bulk NO_3^- and COD were 14 mgN L^{-1} and 3.75 mgCOD L^{-1}, respectively (Figure 3a). The NO_3^- concentration, not shown in Figure 3a, had an almost constant profile due to the lack of donor.

Under anoxic conditions, NO_3^- penetrates deeper into the biofilm (Figure 3c) than when oxic or anoxic conditions in the presence of excess COD were considered (Figures 2a and 2b), because it is not reduced in the interior. The lack of electron donor limits reduction of the two intermediates, NO_2^- and N_2O, which are formed in outer region where little COD and therefore little M_{red} are present. These intermediates also diffuse deeper into the biofilm because they are not reduced. At the outer edge of the biofilm, the decreasing N_2O concentration profile (Figure 3a) shows that N_2O is exported to the bulk. The N_2O flux is around half of that for non-limiting COD conditions described above. This translates into lower emission rates under electron donor limitation, although a greater fraction of the reduced NO_3^- is emitted as N_2O.

The process rates proceed at much lower values than their maximum in the deeper biofilm (Figure 3c), until a depth of 200 μm. The NO_2^- process rate tends to equal that of NO_3^- once NO_2^- starts to accumulate (Figure 3c). The outer portion of the biofilm allows the consumption of NO_3^- (negative net rate) and the formation of the two intermediates, NO_2^- and N_2O (positive net rates), as shown in Figure 3b. Given the limited presence of COD, only the outer biofilm experiences denitrification (Figure 3b). This allows formation of NO_2^- that cannot be reduced further deeper in the biofilm due to lack of donor. In the outer portion, NO_2^- is reduced to N_2O, due to its higher affinity for M_{red}. N_2O then is released to the bulk, leading to N_2O emissions (Figure 3a).

3.5 | Effects of NO_3^-, DO, and biofilm thickness when donor is in excess

This section systematically explores the effects of NO_3^-, DO, and biofilm thicknesses on N_2O production in denitrifying biofilms. All the scenarios were for non-limiting COD concentrations throughout the biofilm. The model was used to assess the effect of bulk NO_3^- and DO on N_2O emission rates per unit reactor volume, for both biofilm and suspended-growth systems. A 5-μm thick "biofilm" was assumed to represent suspended growth, while the 50, 100, and 400-μm cases represented denitrifying biofilms. Note that all biofilms were assumed to have the same area, so the total biomass per reactor volume differed for the different biofilm thicknesses.

With increasing NO_3^- concentration in the bulk, the 5-μm biofilm reached its maximum N_2O production rate at a NO_3^- concentration of around 4 mgN L^{-1} (Figure 4a), because NO_3^- was available throughout the entire biofilm. As expected, due to diffusion limitations, the thicker the biofilm, the higher the NO_3^- concentration needed to reach the maximum bulk N_2O concentration. Also, given the excess donor throughout the biofilm, the interior of the thicker biofilms served as a sink for N_2O formed in the outer regions. This accounts for the lower bulk N_2O concentrations obtained at lower bulk NO_3^- (Figure 4a). The higher volumetric biomass concentration in the reactor at larger biofilm thickness accounts for the higher maximum volumetric rate of N_2O formation.

The effect of bulk DO on N_2O production was also explored as a function of biofilm thickness (Figure 4b). For the 5 μm biofilm, N_2O emissions approached zero as the DO increased above 0.1 mg L^{-1}. However, biofilms with greater thicknesses first increased the N_2O formation then decreased it to low and constant values. This can be explained by a lower reduction of NO_3^- when DO is present. With increasing DO, the greater DO penetration progressively forces denitrification deeper into the biofilm and eventually shuts down all denitrification steps. Note that for most simulations, the bulk NO_3^- concentration was similar to the 14 mgN L^{-1} influent concentration. While this was not true for the 400 μm biofilm, this had a very small impact on the results and the percent of change was negligible.

The percent of N_2O formed per NO_3^- reduced is shown as a function of the bulk NO_3^- concentration in Figure 4c. The 5 μm biofilm had the highest percentage, 5%, and remained essentially constant with the bulk NO_3^- concentration. Greater biofilm thicknesses had lower percentages of N_2O formation, and the amount decreased with increasing bulk NO_3^- concentration. This can be attributed to thicker biofilms having greater N_2O reduction in the deeper regions. However, once NO_3^- is available at non-rate-limiting values in the whole biofilm, there is no longer a "sink" in the deeper regions for N_2O reduction.

In some cases, the reactor influent may contain N_2O from an upstream nitrification or other process. We explored the effect of influent N_2O, both in the presence and absence of NO_3^- (Supplementary Information, Figure S2). As expected, given the high rates of N_2O reduction and its high affinity for electrons, high N_2O consumption fluxes were observed.

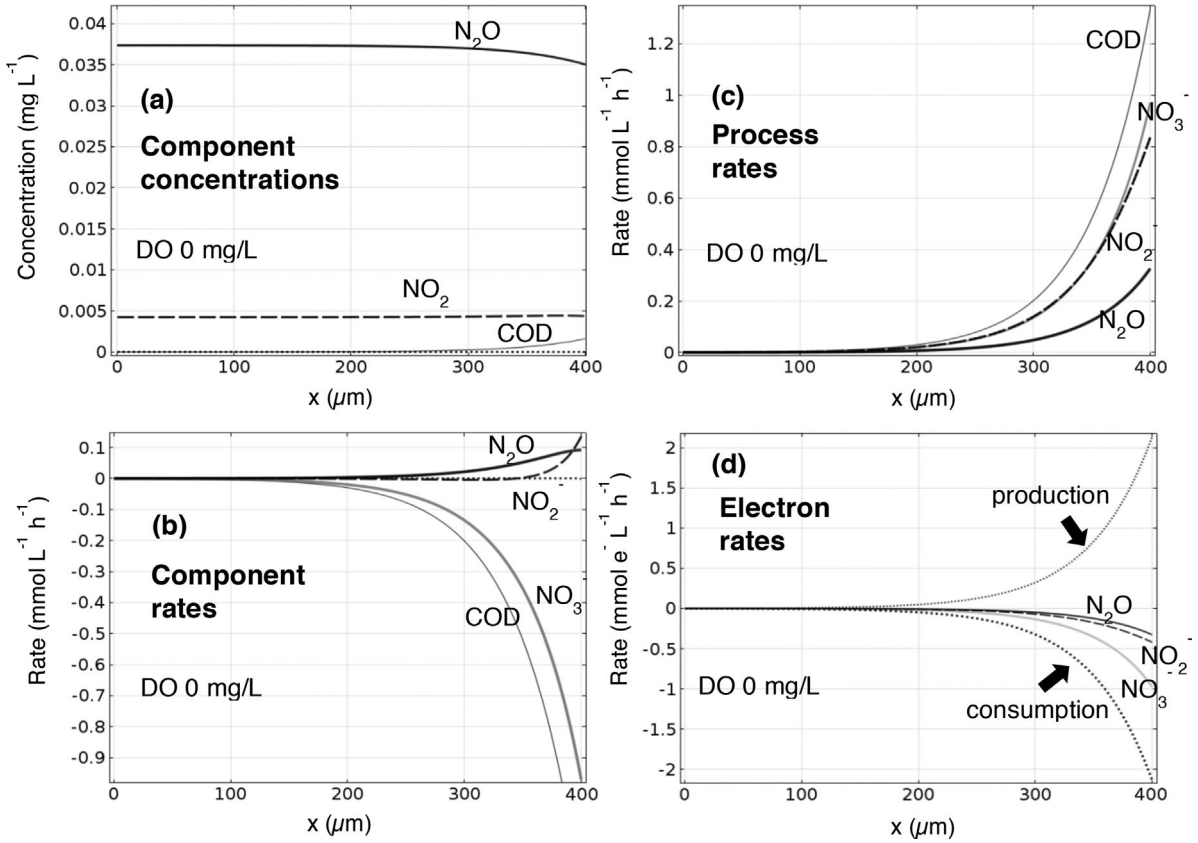

FIGURE 3 Concentration and rate profiles in a 400-μm biofilm with electron donor limitation and an anoxic bulk. Component concentrations (a), net component reaction rates (b), process rates (c), and electron production/consumption rates (d) over the biofilm depth. NO is not shown as it is quickly consumed and maintained at near-zero concentrations

4 | DISCUSSION

These results show the mechanisms of N_2O formation in denitrifying biofilms are different from those in suspended growth processes. In suspended growth systems, all microorganisms are exposed to similar bulk concentrations of both substrates and intermediates. However, biofilms experience substrate gradients, and intermediates formed in one redox zone can diffuse to another (deBeer, Schramm, Santegoeds, & Kuhl, 1997; Nielsen et al., 1990; Sabba et al., 2015). This can impact N_2O formation in several ways. First, N_2O is formed as a denitrification intermediate in the outer biofilm, where NO_3^- and NO_2^- concentrations are higher, but can diffuse and be consumed in deeper regions where NO_3^- and NO_2^- concentrations are lower. Thus, biofilms have regions that can serve as a sink for N_2O, mitigating N_2O emissions (Ni & Yuan, 2013; Ni, Smets, Yuan, & Pellicer-Nacher, 2013). This mechanism is similar to the formation, diffusion, and consumption of hydroxylamine in nitrifying biofilms, as reported by Sabba et al. (2015).

When O_2 is present in the bulk, suspended growth systems would normally not denitrify and therefore not have N_2O formation. However, biofilms may produce N_2O under such conditions. One explanation is the presence of anoxic zones in the deeper biofilm, which allow denitrification. But an additional effect is the diffusion of NO_2^- from the interior toward the exterior of the biofilm. NO_2^- has a higher maximum specific reduction rate than NO_3^- reduction, and also a higher affinity for M_{red} than NO_3^- and N_2O, making it less sensitive to O_2 inhibition. In the biofilm system, NO_2^- can form from deeper in the biofilm where NO_3^- is reduced. It then diffuses to the outer biofilm, where it is reduced in the presence of trace O_2. Since N_2O reduction is inhibited in the presence of O_2, a narrow region of net N_2O formation appears in the outer biofilm, leading to greater N_2O export to the bulk liquid. While these effects may be specific to the parameters from Pan, Ni, and Yuan (2013), the main message is that intermediates can diffuse to different environments within the biofilm, leading to transformations that would not occur where they originated. These effects are unique to biofilms.

The results from this research can provide insights into the behavior of multispecies biofilms, where both nitrifying and denitrifying microorganism are present. In such biofilms, AOB can produce N_2O in zones where the O_2 concentration decreases. If sufficient COD is present, N_2O formed by AOB in the outer regions could be reduced by denitrifying bacteria in the deeper, anoxic regions. This is especially true for membrane-aerated biofilm reactors (MABRs), where a gas-supplying membrane is used to supply DO to the base of a biofilm growing on the membrane outer surface. If the bulk liquid is anoxic, N_2O generated by the inner, nitrifying layer can be reduced in the outer, denitrifying layer.

When the COD concentration is limiting, biofilms may produce more N_2O relative to the amount of NO_3^- reduced. This is consistent

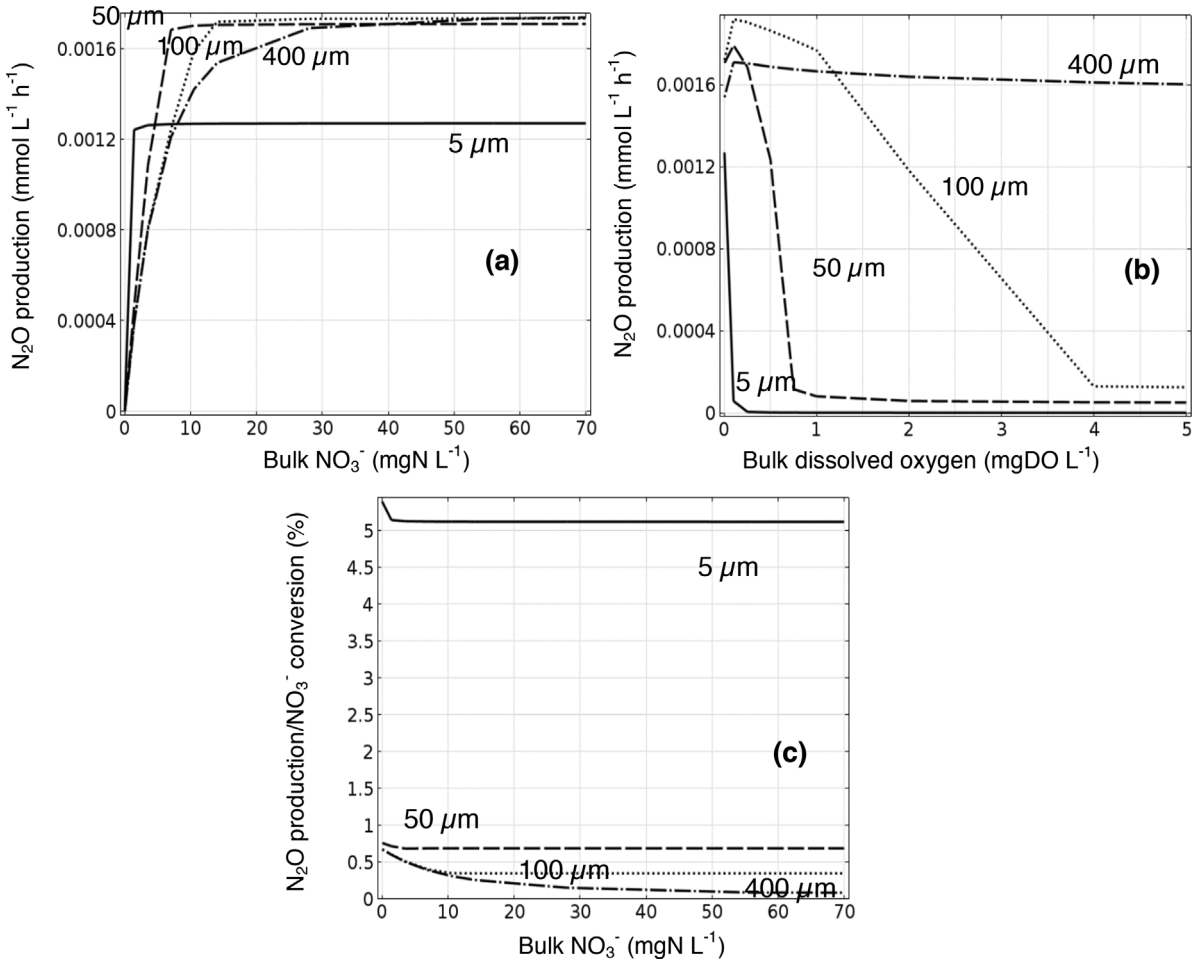

FIGURE 4 N_2O production for biofilms of different thicknesses, per unit reactor volume and time: (a) as a function of bulk NO_3^- in anoxic conditions; (b) as a function of DO at constant NO_3^- concentration. (c) Percent N_2O production from the total NO_3^- reduced as a function of bulk NO_3^- in anoxic conditions

with previous research showing COD limitation can lead to greater emissions (Chung & Chung, 2000; Hanaki, Hong, & Matsuo, 1992; Itokawa, Hanaki, & Matsuo, 2001; Kishida et al., 2004; Law et al., 2012). When N_2O is present in the bulk, it may be scavenged by the denitrifying bacteria, even in the presence of NO_3^- (Pan et al., 2015; Pan, Ni, Bond, et al., 2013; Read-Daily et al., 2016). Our research shows this can also occur in a biofilm, even with an aerobic bulk liquid. For example, if N_2O is produced in an upstream process or by AOB in the outer, aerobic biofilm layer, the underlying denitrifying biofilm can reduce both NO_3^- and N_2O.

5 | CONCLUSIONS

Biofilms are subject to unique mechanisms of N_2O formation and consumption, which result in behavior that differs from suspended growth systems. Substrate gradients and diffusion of intermediates from one redox zone to another can have important impacts. For example, in presence of excess COD, the deeper regions of a denitrifying biofilm allow N_2O consumption. There would be no consumption of N_2O in suspended growth systems, where all microorganisms experience the same environment.

In order to minimize N_2O emission from denitrifying biofilm systems, processes should maintain low bulk NO_3^- concentrations, providing low denitrification rates and therefore low accumulation of N_2O. Also, maintaining low bulk DO values or utilizing thicker biofilms with greater bulk COD allows more N_2O scavenging.

Further research is needed to address the behavior of more complex biofilms containing both nitrifying and denitrifying microorganisms.

ACKNOWLEDGMENTS

F.S. and R.N. were supported by NSF project CBET0954918 (Nerenberg CAREER award) and WERF project U2R10. F.S. received additional support from the Bayer Corporation Fellowship. C.P. work was supported by a Melchor Visiting Professor grant from University of Notre Dame.

CONFLICTS OF INTEREST

The authors declare no competing financial interest.

ORCID

Robert Nerenberg http://orcid.org/0000-0003-2203-5004

REFERENCES

Chung, Y., & Chung, M. (2000). BNP test to evaluate the influence of C/N ratio on N_2O production in biological denitrification. *Water Science and Technology*, *42*, 23–27.

deBeer, D., Schramm, A., Santegoeds, C., & Kuhl, M. (1997). A nitrite microsensor for profiling environmental biofilms. *Applied and Environmental Microbiology*, *63*, 973–977.

Eldyasti, A., Nakhla, G., & Zhu, J. (2014). Influence of biofilm thickness on nitrous oxide (N_2O) emissions from denitrifying fluidized bed bioreactors (DFBBRs). *Journal of Biotechnology*, *192*, 281–290.

Hanaki, K., Hong, Z., & Matsuo, T. (1992). Production of nitrous-oxide gas during denitrification of waste-water. *Water Science and Technology*, *26*, 1027–1036.

Hiatt, W. C., & Grady, C. P. L., Jr. (2008). An updated process model for carbon oxidation, nitrification, and denitrification. *Water Environment Research*, *80*, 2145–2156.

Itokawa, H., Hanaki, K., & Matsuo, T. (2001). Nitrous oxide production in high-loading biological nitrogen removal process under low COD/N ratio condition. *Water Research*, *35*, 657–664.

Kampschreur, M. J., Kleerebezem, R., Picioreanu, C., Bakken, L., Bergaust, L., de Vries, S., . . . van Loosdrecht, M. C. M. (2012). Metabolic modeling of denitrification in *Agrobacterium tumefaciens*: A tool to study inhibiting and activating compounds for the denitrification pathway. *Frontiers in Microbiology*, *3*, 370.

Kampschreur, M. J., Temmink, H., Kleerebezem, R., Jetten, M. S. M., & van Loosdrecht, M. C. M. (2009). Nitrous oxide emission during wastewater treatment. *Water Research*, *43*, 4093–4103.

Kishida, N., Kim, J., Kimochi, Y., Nishimura, O., Sasaki, H., & Sudo, R. (2004). Effect of C/N ratio on nitrous oxide emission from swine wastewater treatment process. *Water Science and Technology*, *49*, 359–365.

Law, Y., Ye, L., Pan, Y., & Yuan, Z. (2012). Nitrous oxide emissions from wastewater treatment processes. *Philosophical Transactions of the Royal Society B-Biological Sciences*, *367*, 1265–1277.

Lu, H., & Chandran, K. (2010). Factors promoting emissions of nitrous oxide and nitric oxide from denitrifying sequencing batch reactors operated with methanol and ethanol as electron donors. *Biotechnology and Bioengineering*, *106*, 390–398.

Ni, B., Ruscalleda, M., Pellicer-Nacher, C., & Smets, B. F. (2011). Modeling nitrous oxide production during biological nitrogen removal via nitrification and denitrification: Extensions to the general ASM models. *Environmental Science & Technology*, *45*, 7768–7776.

Ni, B., Smets, B. F., Yuan, Z., & Pellicer-Nacher, C. (2013). Model-based evaluation of the role of Anammox on nitric oxide and nitrous oxide productions in membrane aerated biofilm reactor. *Journal of Membrane Science*, *446*, 332–340.

Ni, B., & Yuan, Z. (2013). A model-based assessment of nitric oxide and nitrous oxide production in membrane-aerated autotrophic nitrogen removal biofilm systems. *Journal of Membrane Science*, *428*, 163–171.

Nielsen, L., Christensen, P., Revsbech, N., & Sorensen, J. (1990). Denitrification and oxygen respiration in biofilms studied with a microsensor for nitrous-oxide and oxygen. *Microbial Ecology*, *19*, 63–72.

Pan, Y., Ni, B. J., Lu, H., Chandran, K., Richardson, D., & Yuan, Z. (2015). Evaluating two concepts for the modelling of intermediates accumulation during biological denitrification in wastewater treatment. *Water Research*, *71*, 21–31.

Pan, Y., Ni, B., Bond, P. L., Ye, L., & Yuan, Z. (2013). Electron competition among nitrogen oxides reduction during methanol-utilizing denitrification in wastewater treatment. *Water Research*, *47*, 3273–3281.

Pan, Y., Ni, B., & Yuan, Z. (2013). Modeling electron competition among nitrogen oxides reduction and N_2O accumulation in denitrification. *Environmental Science & Technology*, *47*, 11083–11091.

Ravishankara, A. R., Daniel, J. S., & Portmann, R. W. (2009). Nitrous oxide (N_2O): The dominant ozone-depleting substance emitted in the 21st century. *Science*, *326*, 123–125.

Read-Daily, B. L., Sabba, F., Pavissich, J. P., & Nerenberg, R. (2016). Kinetics of nitrous oxide (N_2O) formation and reduction by Paracoccus pantotrophus. *AMB Express*, *6*, 85.

Sabba, F., Picioreanu, C., Boltz, J. P., & Nerenberg, R. (2016). Predicting N_2O emissions from nitrifying and denitrifying biofilms: A modeling study. *Water Science & Technology*, *75*, 530–538. https://doi.org/0.2166/wst.2016.484

Sabba, F., Picioreanu, C., Perez, J., & Nerenberg, R. (2015). Hydroxylamine diffusion can enhance N_2O emissions in nitrifying biofilms: A modeling study. *Environmental Science & Technology*, *49*, 1486–1494.

Schreiber, F., Polerecky, L., & de Beer, D. (2008). Nitric oxide microsensor for high spatial resolution measurements in biofilms and sediments. *Analytical Chemistry*, *80*, 1152–1158.

Sutka, R., Ostrom, N., Ostrom, P., Breznak, J., Gandhi, H., Pitt, A., & Li, F. (2006). Distinguishing nitrous oxide production from nitrification and denitrification on the basis of isotopomer abundances. *Applied and Environmental Microbiology*, *72*, 638–644.

Vilar-Sanz, A., Puig, S., Garcia-Lledo, A., Trias, R., Dolors Balaguer, M., Colprim, J., & Baneras, L. (2013). Denitrifying bacterial communities affect current production and nitrous oxide accumulation in a microbial fuel cell. *PLoS ONE*, *8*, e63460.

von Schulthess, R., Kuhni, M., & Gujer, R. (1995). Release of nitric and nitrous oxides from denitrifying activated-sludge. *Water Research*, *29*, 215–226.

von Schulthess, R., Wild, D., & Gujer, W. (1994). Nitric and nitrous oxides from denitrifying activated sludge at low-oxygen concentration. *Water Science and Technology*, *30*, 123–132.

Wicht, H. (1996). A model for predicting nitrous oxide production during denitrification in activated sludge. *Water Science and Technology*, *34*, 99–106.

Wild, D., von Schulthess, R., & Gujer, W. (1994). Synthesis of denitrification enzymes in activated-sludge—Modeling with structured biomass. *Water Science and Technology*, *30*, 113–122.

Wu, G., Zheng, D., & Xing, L. (2014). Nitritation and N_2O emission in a denitrification and nitrification two-sludge system treating high ammonium containing wastewater. *Water*, *6*, 2978–2992.

Zumft, W. G. (1997). Cell biology and molecular basis of denitrification. *Microbiology and Molecular Biology Reviews*, *61*, 533.

SUPPORTING INFORMATION

Additional Supporting Information may be found online in the supporting information tab for this article.

How to cite this article: Sabba F, Picioreanu C, Nerenberg R. Mechanisms of nitrous oxide (N_2O) formation and reduction in denitrifying biofilms. *Biotechnology and Bioengineering*. 2017;114:2753–2761. https://doi.org/10.1002/bit.26399